A Solar Energetic Particle Spectrometer (SEPS) Concept

Mark Christl*, James H. Adams Jr.*, Evgeny N. Kuznetsov†, Samah Nazzel†, Thomas A. Parnell†, and John W. Watts †
*NASA Marshall Space Flight Center
†University of Alabama in Huntsville

***Abstract*. An outstanding problem of solar and heliospheric physics is the transport of solar energetic particles. The more energetic particles, those arriving early in the event can be used to probe the transport processes. The arrival direction distribution of these particles carries information about scattering during their propagation that can be used to test models of interplanetary transport. Also, of considerable importance to manned missions is the dose that the crews experience during an intense solar particle event, as well as the risk to space systems. A recent study concludes that 90% of the absorbed skin dose results from particles in the energy range 20-550 MeV[1]. We will describe a new compact detector concept that would cover the energy range from 50-600 MeV with a single detector. This energy range has been difficult to cover and only limited data, generally available only in broad energy bins, are available from a few past and present instruments. The SEPS concept could provide improved measurements for this energy range.**

***Keywords*: cosmic rays, SEP , detector**

I. Introduction

The solar energy particle (SEP) flux and spectra contain important information about the seed population, the acceleration processes and the transport in the heliosphere. High energy SEPs are accelerated close to the sun and during the initial stages of Solar Particle Events (SPEs). The highest energy particles arriving at distances of 1 A.U. are quasi-collimated with measurable angular anisotropies. As they proceed beyond 1 A.U. some are scattered in the outer heliosphere and return to 1 A.U., delayed with respect to the original wave, with modified angular and energy distributions. These particles contain signatures of scattering processes that can be revealed by the high energy SEP flux.

These SEP are also critical in NASAs exploration program. A recent study concludes that 90% of the absorbed skin dose results from particles in the energy range 20-550 MeV [1]. Doses to internal organs will extend the energy range. Together with the unpredictable occurrence of such events, the spectra and time evolution of events are not predictable at this time. Consequently, they are a concern for future manned missions outside the geomagnetic field.

Satellites outside the geomagnetic field routinely carry low energy particle detectors that work up to ≈ 50 MeV and are capable of tolerating elevated particle rates seen during solar out bursts. At energies approaching 1 GeV, the proton flux can be monitored through ground level enhancements (GLEs) by measuring the neutron flux produced in the atmosphere through proton interacts. GLEs are detected with less than 20% of the SPEs [2]. The energy range between spectrometers in space and neutron monitors on the ground has limited data and planned future missions do not yet fully address the need. Present and past instruments have relied on multiple detection methods and techniques and multiple sets of particle telescopes; each with a limited range of energies and angles. The concept that is described here combines two detection techniques in a single compact detector.

Property	CZ	CsI(Tl)
Density(g/cc)	5.9	4.5
Index of refraction	2.15	1.79
Cherenkov Threshold (MeV)	125	190
Max. Cherenkov Angle	62°	56°
Absorption/cm	5%	small

Table 1. Physical properties of CZ and CsI materials.

II. Detector Concept

The goal is to fill gaps and improve the quality in SEP data. We employ high-density optical materials with high refractive index, which also has a scintillation component, as a combination Cherenkov-Scintillation detector. We have studied two materials, Cubic Zirconia (CZ) and Cesium Iodine (CsI), so far in this investigation. The physical properties of these materials are listed in Table 1.

Scintillation in the detector closely follows the energy loss of the incident particle. The scintillation signal is not necessarily linear but is monotonically increasing with energy deposited. In the case of the CZ, which is not generally considered a scintillator, the scintillation efficiency is small. CsI is an efficient scintillating material with well known scintillation properties [3].

Cherenkov radiation energy threshold and yield depends on the index of refraction of the material. For

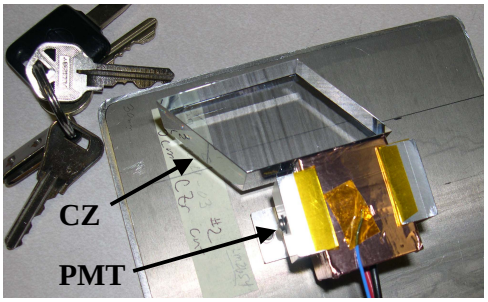

Fig. 1: CZ detector with PMT.

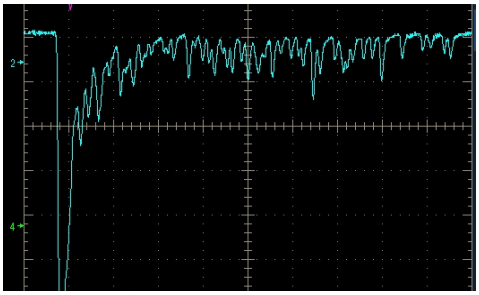

Fig. 2: Oscilloscope trace of a single event. The timescale is 80ns/div (800ns full trace). Each of the small peaks in the tail are consistent with single photoelectron signals.

our concept it is desirable to have a threshold of approximately 200 MeV so materials with high index of refraction are being studied. A high refractive index also lends itself to efficient photon collection through total internal reflection and smaller losses at boundaries. Four characteristic of the Cherenkov radiation are important in this application: prompt emission, number and directionality of the emitted photons, and optical spectra.

Different approaches may be used to separate the scintillation and Cherenkov signals in the materials. In CZ the total number of scintillation photons produced is only a few times more than that typically detected by Cherenkov detectors, and it has a scintillation decay time of microseconds. Together these two characteristics permit separating the prompt Cherenkov signal from the slower scintillation response. For CsI the scintillation photons greatly exceed the Cherenkov signal and it has a long scintillation decay time. However, the CsI has a discernable rise time before the scintillation peaks. This rise time is of the order of $\sim$20 ns [3] and is sufficient to detect the prompt Cherenkov signal prior to any significant scintillation.

III. Tests

We have tested 4 CZ samples with different geometry at the Indiana University Cyclotron Facility (IUCF) using proton beams with energy from 50 to 205 MeV. Two of the CZ samples have cross sections of a parallelogram of dimensions 2.5 cm and 4.2 cm (Figure 1). The other 2 CZ samples are cuboids with dimension 2x3x3 cc and

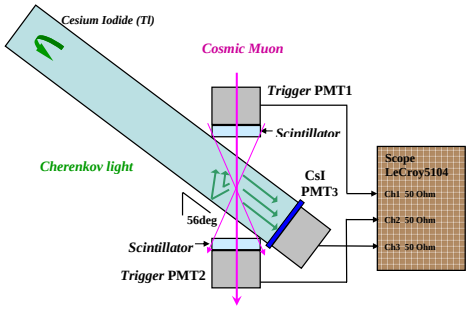

Fig. 3: Experimental setup for CsI to detect muons. The angle between the CsI principal axis and the average muon trajectory is 56°.

3x3x5 cc. Each radiator was bonded to a PMT using optical cement. A thin reflective coating was applied to the surface opposite the PMT to improve the collection of Cherenkov photons. The detectors were mounted in a light tight box. A 1.0 mm thick silicon detector was placed behind the test articles to measure the ionization rate of particles exiting the crystals. Proton data was acquired with the particle paths parallel to the PMT window for all the detectors. For the two cuboids, data was also acquired with the proton paths perpendicular to the PMT windows. A PMT with plastic scintillator was used as a trigger for the data acquisition system. The event rates range between 1-3 kHz and a 1 cm diameter collimator was used to insure the protons were incident near the center of the detector. An oscilloscope trace of a single event in the CZ is shown in Figure 2.

The CsI(Tl) has been tested using ground-level muons and tests are planned at the IUCF in the near future. The test setup is shown in Figure 3 and includes 2 trigger PMTs with plastic scintillators to restrict the trajectory of muons used in the analysis. The output of the CsI was studied using two optical filters: BG3 and CZ that provide some information about the spectral characteristics. Several different exposures were completed using muons. The location of the two trigger scintillators was varied for each exposure to study the angular dependence of the prompt signal and the photon signal attenuation along the axis of the CsI. The prompt peak was maximized when the average angle between the muon trajectory and the CsI axis was 56°. An oscilloscope trace of a single event in the CZ is shown in Figure 4.

IV. Results

We have analyzed the decay time and scintillation efficiency for two of the CZ samples. The time structure of the scintillation signal shows two principal components that we fit with separate exponential decay functions with time constants of 0.1 microsecond and 1.0 microsecond. The full scintillation signal is nearly equally divided between these two components. The analysis of the scintillation efficiency for two different

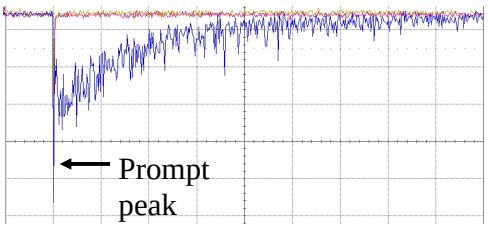

Fig. 4: Oscilloscope trace of a muon generated signal in CsI. The timescale is 500 ns/div. The large prompt peak is due to Cherenkov photons.

CZ crystals shows an efficiency of 3 to 4 photons per MeV of energy deposition. This is a low efficiency by normal scintillation detector standards. The data in Figure 5 shows the detected signal for one of the CZ samples along with the results of the analysis that permit separating the two components that are shown as continuous lines. The sharp peak in the scintillation signal is due to protons whose range is equal to the depth of the CZ sample. The rise in signal at high energy is due to the detection of Cherenkov photons.

A spectral analysis of the scintillation produced in CZ has not yet been investigated. We expect that the scintillation is produced by trace amounts of contaminates that are included during the manufacturing of the CZ samples. Upon further investigation, the scintillation efficiency may be tailored to this application.

The CsI(Tl) is known to have multiple scintillation components and pure CsI is known to have very fast decay times on the order of 20 nanoseconds [3]. The sample we used has a bulk decay time of 1 microsecond as measured using relativistic muons. If any prompt scintillation is present in the muon data it appears to be small since the prompt signal is almost entirely accounted for by the estimated strengthens of the Cherenkov signal and the rise time component of the main scintillation pulse. A more careful analysis of the early scintillation process for our specific sample is planned for an upcoming exposure with protons at the IUCF.

The averaged response to relativistic muons in CsI is shown in Figure 6. The Cherenkov signal is evident for both test conditions displayed that show a prompt peak on the slow rising scintillation signal. The dark trace was acquired with the trigger scintillators positioned close to the PMT and with vertical muon trajectories (Figure 3). The lighter trace was acquired with the setup rotated 180° about the axis normal to the page. In this configuration, photons emitted at 56° to the vertical must be reflected from the far end of the crystal, opposite the PMT, before being detected. The time shift between the two peaks is 3 ns, the delay expected from photons that are reflected from the opposite end of the CsI detector. The characteristic emission angle for the Cherenkov signal was confirmed by selectively analyzing muons with varying trajectories through the crystal. These tests confirmed that the prompt pulse was

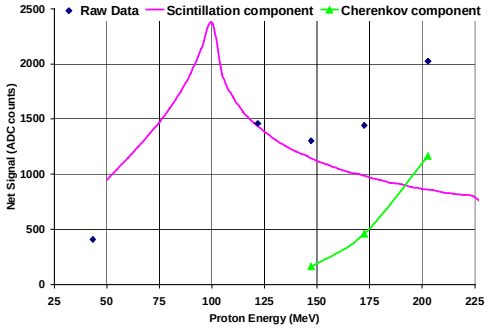

Fig. 5: Raw data and analysis results for the CZ detector exposed to protons at 50, 125, 150, 175 and 205 MeV. The two curves show the scintillation and Cherenkov components of the total signal separately.

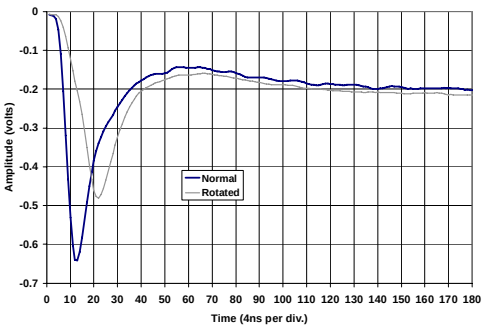

Fig. 6: Average response for muons in the CsI. The two peaks are due to Cherenkov photons directly incident on the PMT and those reflected from the far end of the CsI log. The long tail shows the delayed response of the primary scintillation. The two traces are for different setups (see text). The timescale is 4ns/div (73 ns full trace).

not isotropic and showed a maximum signal consist with a directed emission 56° from the axis of the muon trajectory. We further confirmed that the absorption in the CsI was small and photons reflected from the far surface, opposite the PMT, were efficiently detected. Introducing two different filters, BG3 and CZ, we observed higher Cherenkov/scintillation ratio since these filters attenuate the longer wavelength signals more.

V. Future Work

We plan further exposures of test samples with muons and particle beams. The application of a dual scintillator/Cherenkov detector in a particle spectrometer for SEPs will require selecting the scintillation and Cherenkov properties in terms of relative light yields and decay times that are useable with anticipated particle fluxes.

References

[1] Adams Jr.,J.H.,Watts J.W.,"The Solar Proton Energy Ranges that Contribute to Crew Absorbed Dose.", 38th COSPAR Scientific Assembly, Beijing, China, (2006).

[2] Shea,M.A., Smart, D.F., ”Significant Solar Proton Events For Five Solar Cycles (1954-2007)”, ICRC31 (Merida), Vol 1, pg 261,(2007)
[3] Knolls, G. F., Radiation Detection and Measurement, Wiley 3rd Ed.,(1999)